J Opt
https://doi.org/10.1007/s12596-024-02111-6

RESEARCH ARTICLE

Analysis of point and linear defects inside photonic crystals with square and hexagonal lattices for communication applications

Miami Mohammed[1] · Ahmad K. Ahmad[2]

Received: 11 December 2023 / Accepted: 24 July 2024

Abstract In the current study, we were theoretically able to determine the main difference between the point defect and linear defect of both square and hexagonal photonic lattices. For the point defect, the mode is trapped No matter where in the band structure its frequency falls. The mode of the linear defect is localized to one-direction propagation along with the defect, functioning as a propagation channel rather than as an area-trapping light source. When creating a point defect inside a bandgap, the electric field amplitude is broad and concentrated around the defect region and decays quickly as we move away from the site of the defect. While creating a line defect inside the bandgap, the amplitude of the electric field will continue to propagate in one direction to the end of the path of the line defect within the photonic crystal bandgap. Photonic integrated circuits based on photonic crystals are very important in the improvement of optical communication.

Keywords Photonic crystal · Point defect · Linear defect · Optical communication · Multiplexer · Demultiplexer

Introduction

The periodic dielectric structures are represented by photonic crystals (PCs), which, because of the way light operates in them, were given the label photonic crystal [1, 2]. Since PCs may reflect or trap light, they provide unprecedented levels of control and manipulation of light propagation in the microwave regime, which has sparked an increase in scientific interest in recent years [1–3]. Numerous two-dimensional photonic crystal applications focus on optical integrating devices, such as splitters [4], resonant cavities [5–7], waveguides [1, 8, 9], and waveguide bends [8–11]. These optical devices are crucial for the growth of photonic and electrical circuits. The fascinating property of photonic structures makes it possible to change the band structure's shape (e.g., making it square or hexagonal with circle rods to regulate frequencies that can approach kilohertz or megahertz) or structural parameters (e.g., rod radius, periodicity, and material) [10]. Additionally, the ability to alter the photonic lattice's periodic structure by adding various types of defects, such as local resonant cavities and waveguide modes like this structure, allows for a significant expansion of photonic crystal applications [3, 8, 10]. The electromagnetic wave can be guided by its direction using waveguiding and bending modes [1, 8]. It is challenging to bend a photonic structure, though, unless the bend's radius is much larger than its wavelength. This is because a significant amount of light is wasted. The lack of area needed for large-radius bends is a serious obstacle to the development of integrated optical "circuits" [11, 12].

As an alternative, an extremely sharp, low-loss bend in the waveguides trapped inside a photon crystal might greatly increase the integration's density [12].

COMSOL program (version 5.5) is one of the most important tools for developing a full simulation of the propagation of electromagnetic waves (solution of Maxwell equations) via photonic crystals. In a study on the infinite periodic` photonic crystal, the Bloch bandgap mode structure of a regularly perforated sheet was theoretically investigated

✉ Ahmad K. Ahmad
ahmad.ahmad@nahrainuniv.edu.iq

Miami Mohammed
dr.miamiph@uomustansiriyah.edu.iq

[1] Department of Physics, College of Science, University of Mustansiriyah, Baghdad, Iraq

[2] Laser and Optoelectronics Engineering Department, College of Engineering, Al-Nahrain University, Baghdad, Iraq

Published online: 06 August 2024

by applying COMSOL program. [13]. A different approach is to use the COMSOL MULTIPHYDICS-based finite element method (FEM) to theoretically analyze how an electromagnetic wave flows through a photonic crystal's hexagonal lattice and evaluate the band structure [14]. Computational research using plane wave expansion (PWE) to investigate the photonic bandgap through the transmission of pressure waves generated by sound in photonic crystals square lattice [10]. The finite-difference time-domain (FDTD) approach is used to study the flat-band lattice [15]. Theoretical investigations include defect states inside the photonic crystal's bandgap, which were thoroughly explored in [1, 16]. Analyzing the photonic crystals band structure with hexagonal and square lattices in dielectric materials, Also, evaluating the resonant cavities and the point defects for both lattices' inner bandgap by utilizing the FEM, the PWE method [3], and the FDTD method [2], in addition to defect states in photonic crystals. Furthermore, use the multiple beam interference approach to experimentally analyze the photonic lattice defect in the LiNbO3 photo-refractive crystal [17]. The numerical implementation of FDTD was used to build the photonic crystal and generate a five-channel resonant ring, which is useful in demultiplexer applications. [18]. This was done based on the analysis of the optical channel drop filter. Additionally, photonic crystal analysis was done using the same numerical approach as 2D optical multiplexing devices, which was beneficial. With an incredibly quick conversion speed, the structure is very compactly constructed [19]. Square lattice photonic crystals composed of a rod of silicon and a background consisting of air are used in the creation of a compact 2×1 optical multiplexer for photo processing devices [20]. A 2D photonic crystal was developed using PWE and FDTD techniques to operate as a base for all optical half subtractors [21, 22]. Moreover, FDTD and PWE techniques are employed in the creation of a 2D photonic crystal with a hexagonal lattice that functions as a decoder and produces a 2×4 optical system based on a threshold switching mechanism and Kerr effect [23]. Additionally, a 2D photonic crystal was created by PWE and FDTD methods utilizing rods formed of a dielectric material—such as GaAs—that were submerged in an air background. Based on the nonlinear Kerr's effect, this photonic crystal functions as a nonlinear logic gate [24]. P. Sharan et.al. designed and analysed a two-dimensional photonic crystal based sensor for three different biosensing applications, including measuring the normal and abnormal levels of uric acid, glucose, and creatinine in the blood [25]. M.K. Chhipa et.al. [26–29] also used the FDTD and the PWE methods for design of a 2D PC's ring resonator and Channel Drop Filter (CDF) for optical communication networks.

By evaluating various defect states and the optical characteristics of periodic photonic crystals in dielectric materials for multiplexers-demultiplexer applications that are beneficial for networks optical communication, Our approach is innovative because it can be used to engineer faults in square and hexagonal photonic crystals to provide multiplexing and demultiplexing functions.

The distinct characteristics of these lattice structures and faults provide precise control over signal separation and manipulation as well as a wide range of design possibilities.

Overall, by enabling effective and selective multiple signal extraction, separation, and transmission in optical communication systems, the utilization of point and linear defects within photonic crystals with square and hexagonal lattices adds innovation to multiplexer and demultiplexer applications.

Theory

First, we try to analyze the band structure for two-dimensional square and hexagonal lattices, using COMSOL MULTIPHYSICS Software simulation to investigate the wave propagation in two- dimensional a photonic crystal, photonic bandgap structure (eigenvalue analysis) of the periodic square and hexagonal lattice are analyzed by FEM (real space). The frequencies of Bloch waves are obtained from the eigenvalue solver with wave vector. The change in the wave vector results in dispersion relation from the bandgap structure. The mathematical basis of propagation of the electromagnetic wave in two-dimensional photonic crystal via an inhomogeneous medium can be described by Maxwell's equations [3, 12]. Assuming that the transversal electric (TE) is a linear combination of the electric field, where the photonic crystal plane is perpendicular to the electric field [3]. Maxwell's equations- Helmholtz equation for the electric field that propagates in the photonic crystal is given by [12, 16]:

$$\nabla \times \varepsilon_r^{-1}(\nabla \times E) - \kappa_0^2\left(\varepsilon_r - \frac{j\sigma}{\omega\varepsilon_r}\right)E = 0 \tag{1}$$

where $k_0 = \omega/c$, ω is the incident electric field angular frequency on the crystal and c is the space of light in free-space, the wavelength is $\lambda = j\omega + \delta$, The photonic crystal relative dielectric constant for inhomogeneous structure is $\epsilon_r = (n - ik)^2$. Assuming non-conducting, non-magnetic photonic crystal, then $\mu_r = 1$ and $\sigma = 0$. The wave vector κ for the propagation wave is given by:

$$E(x, y, z) = \tilde{E}(x, y)E_z \exp(-i\kappa_z z) \tag{2}$$

where E_z elucidate the z-component of the electric field at the position ($\vec{r} = x, y, z$). Any electromagnetic simulation must include boundary conditions at the interfaces that are represented by perfect electric conductor (PEC) boundary

conditions. These boundary conditions serve as a mirror for the simulation domain and are provided by:

$$\hat{n} \times \vec{E} = 0 \tag{3}$$

where $\hat{n}$ represents the unit vector that is perpendicular to the simulation domains at all points outside the surface. The periodic condition of photonic crystal lattice is feature by Floquet periodicity of Bloch's theorem.

Design methodology, simulation results and discussion

The first structure we modeled is a 2D photonic crystal structure unit cell square lattice. Assuming the photonic crystal is formed of insulating GaAs circles with radius r = 0.065 µm that occupy the air square lattice centers with lattice constant a = 0.365 µm. As we can see in Fig. 1a, for a given frequency range known as the band gap, the relationship between the wave number and the frequency of the light landing on the photonic crystal is determined by the distance between the pillars. This prevents the light from spreading inside the crystal. The photonic crystal's light frequency is determined by examining the unit cell's period. Regarding Fig. 1b, very few wave vectors that cover the boundaries of the fundamental first Brillouin zone (1BZ) is included in the square lattice's unit cell. One can trace the 1BZ symmetry points from Γ to X to M and back to Γ. We investigated the eigenfrequency of the electromagnetic wave model, Doman frequency, utilizing COMSOL SOFTWARE PROGRAMM. We put the boundary condition at the interfaces is selected as a perfect electric conductor (PEC) to avoid unphysical reflections. Then we put the periodic condition of the square lattice by using the Floquet Bloch wave vector periodicity at the boundary for wave vectors kx and ky. Using meh elements (mesh free triangular) with finer mesh physics-controlled, as shown in Fig. 1c. From the simulation results, As seen in Fig. 2a–c, we determined the five eigenvalues of the z-component of the electric field (E_z) for the transversal electric polarization (TE) of the first Brillouin zone (1Bz) in the square lattice unit cell. The frequency of the Bloch waves is determined from the solution of the eigenvalues. Problems with changing the wave vector with frequency result in dispersion relation which forms the band diagram of square lattice unit cell, as seen in Fig. 2d. Displaying the first five lower bands demonstrates the absence of any electromagnetic waves (i.e., a state of no frequency range propagation) between the third and fourth bands. As a result, this region is characterized as a photonic crystal bandgap at the symmetry points represented by Γ, X, and M.

The second structure, we modeled unit cell of two-dimensional photonic crystal structures for hexagonal lattice, by following the same steps the previous way of unit cell of

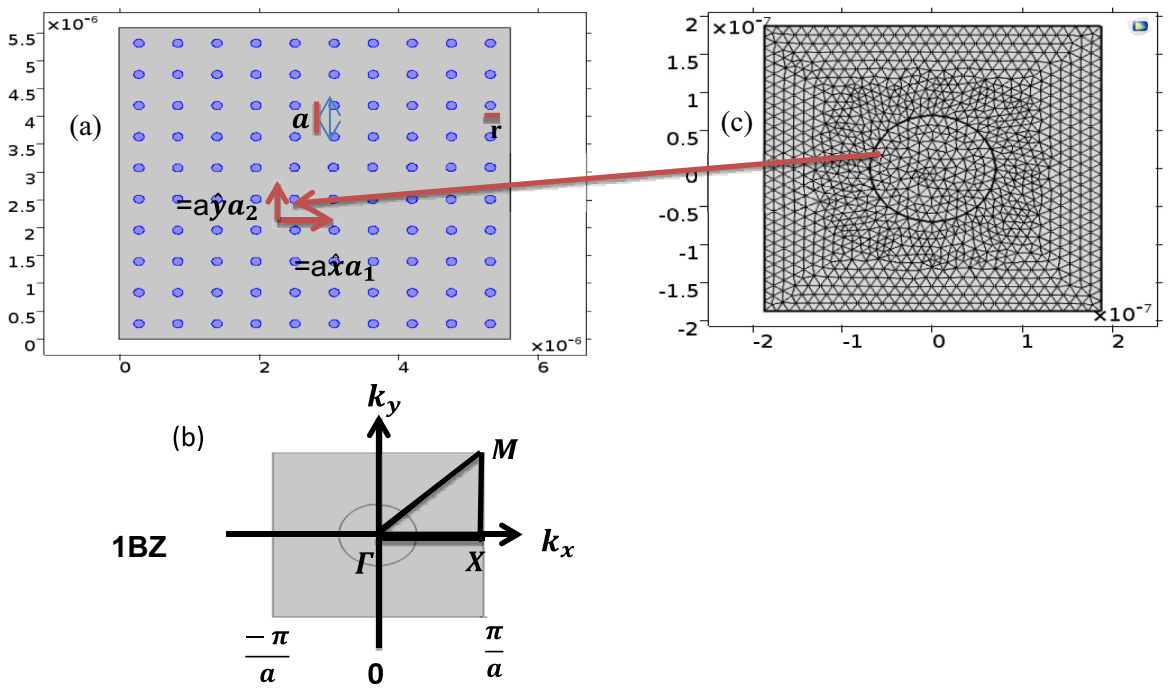

Fig. 1 Using COMSOL software to model the unit cell of a square lattice (**a**), the special symmetry points Γ, X, and M of the 1st BZ unit cell of a square lattice (**b**). Free triangular mesh of unit cell (**c**)

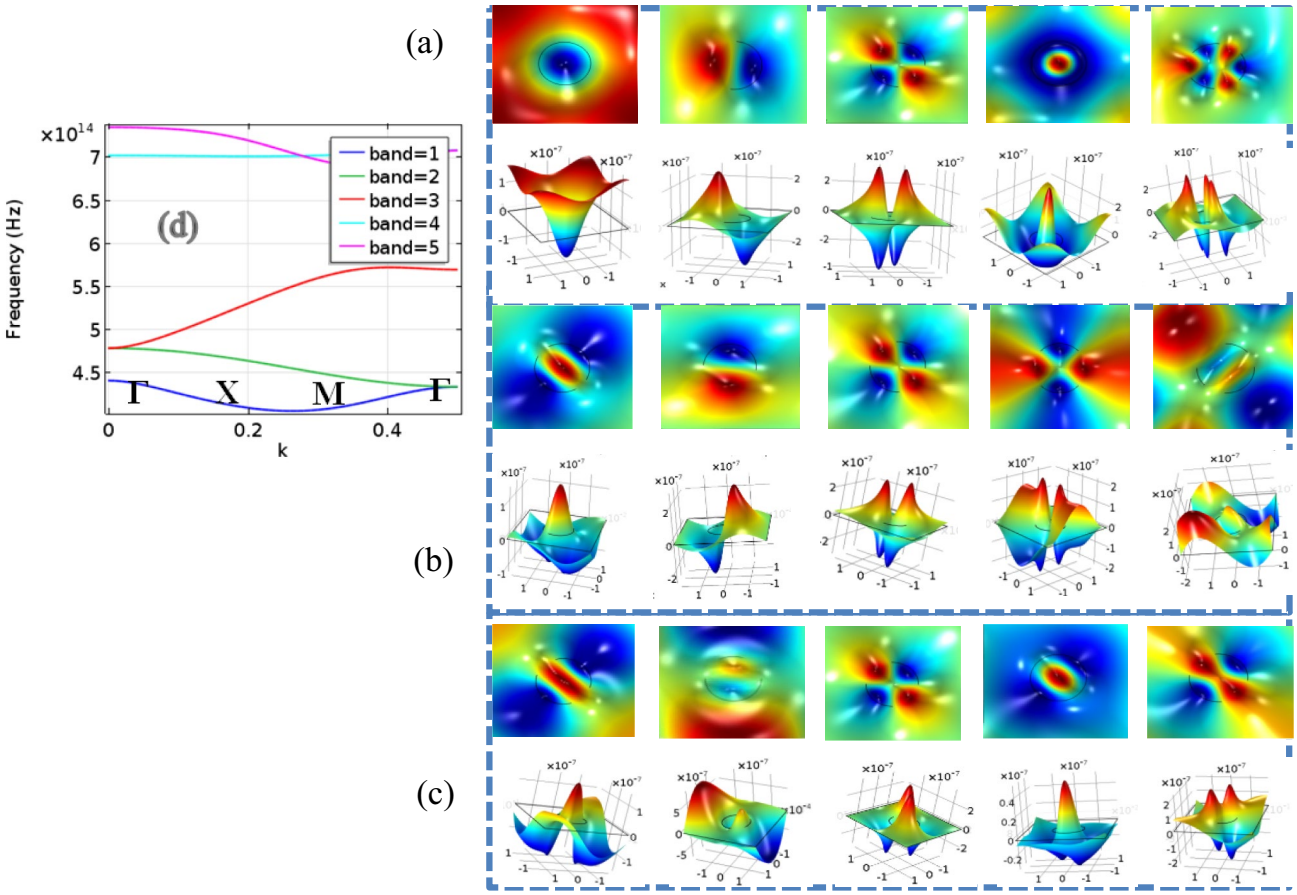

Fig. 2 Contour: distribution of Electric field norm (V/m) for first the five eigenvalues of E_z modes in the unit cell for special symmetry points Γ, X and M (**a–c**), and in (**d**) the dispersion relation (**b** and diagram) of frequency as function the wavenumber k after swept from 0 to 0.5, show five photonic bands of unit cell in the square lattice. There is a frequency range that corresponds to a bandgap in the structure that is limited between the band three and band four; there is no propagation of Bloch waves in this range

square lattice but geometry varies to hexagonal lattice, as shown in the Fig. 3. From the simulation results, we found the five eigenvalues of *z*-component of the electric field (E_z) for the transversal electric polarization (TE) of the hexagonal lattice unit cell first Brillouin zone, as presented in the Fig. 4. Although there is overlap inside the bands between the five and four bands, it is still possible to see us clearly on the band diagram, demonstrates that there is no Bloch wave propagation in the bandgap-corresponding frequency range.

Defect states in two-dimensional square and hexagonal periodic of photonic crystal

After modeling the bandgap structure of the complete structure photonic crystal, as is known, there are no modes allowed within the bandgap structure; the density of the states denoting the number of available modes per unit frequency is zero (this means reflects the light of certain frequency). Trying to break the periodic symmetry of the lattice by perturbing the lattice creating a defect in the structure of photonic crystal, such as point or line defects by removing single rod to create a single localized mode or by removing set of closely rods guide for the light frequencies inside the bandgap of the photonic crystal structure [1, 12], such these defects are especially important for telecommunication application that allows one to localized light about these defects within the bandgap of photonic crystal [3]. By eliminating a single rod from the square lattice, we produce a cavity point that is essentially surrounded by reflecting walls; such a cavity is important for controlling light and localized one mode within bandgap with a narrow frequency range, shows the light bounces in the defect area, trapped by surrounding bandgap, the light cannot leakage because of bandgap and we can localize the mode to the defect area [1, 3].

There could be a linear flaw. By altering a linear unit cell, it is possible to guide light from one place to another. The goal is to create a waveguide from a perfect photonic crystal by modifying the linear defects in a unit cell. Then, the light

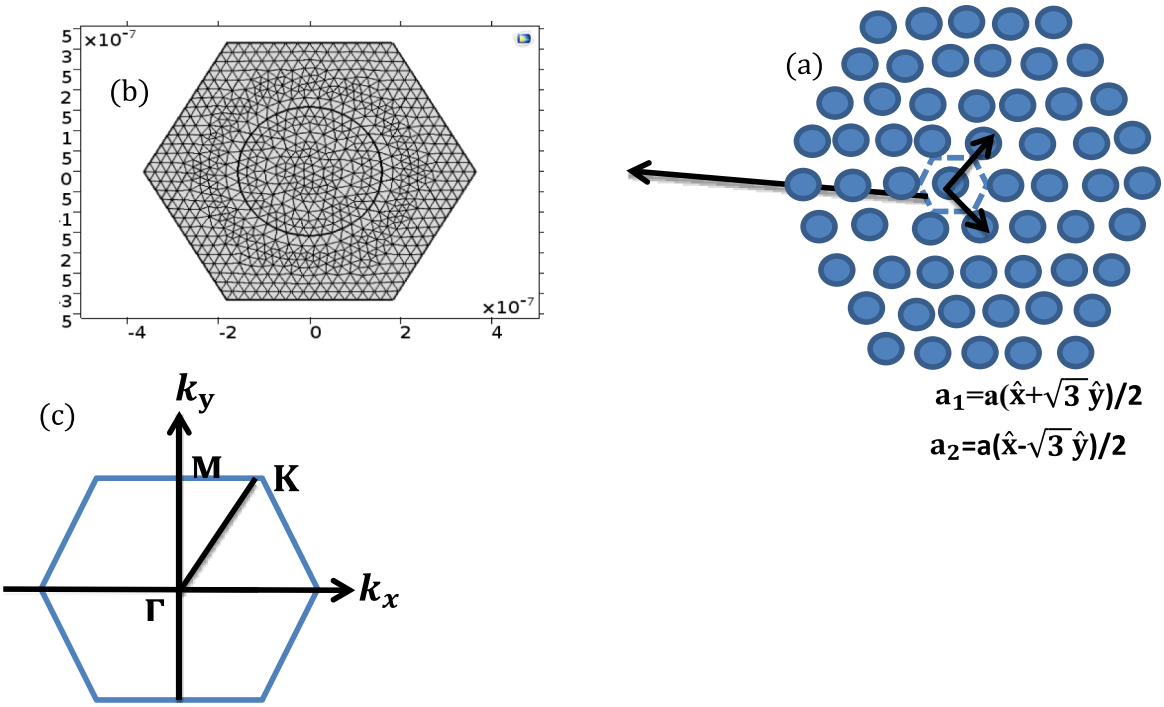

Fig. 3 **a** COMSOL software modelling the unit cell of hexagonal lattice, **b** free triangular mesh of unit cell, **c** the special symmetry points Γ, M, and K of the hexagonal lattice unit cell

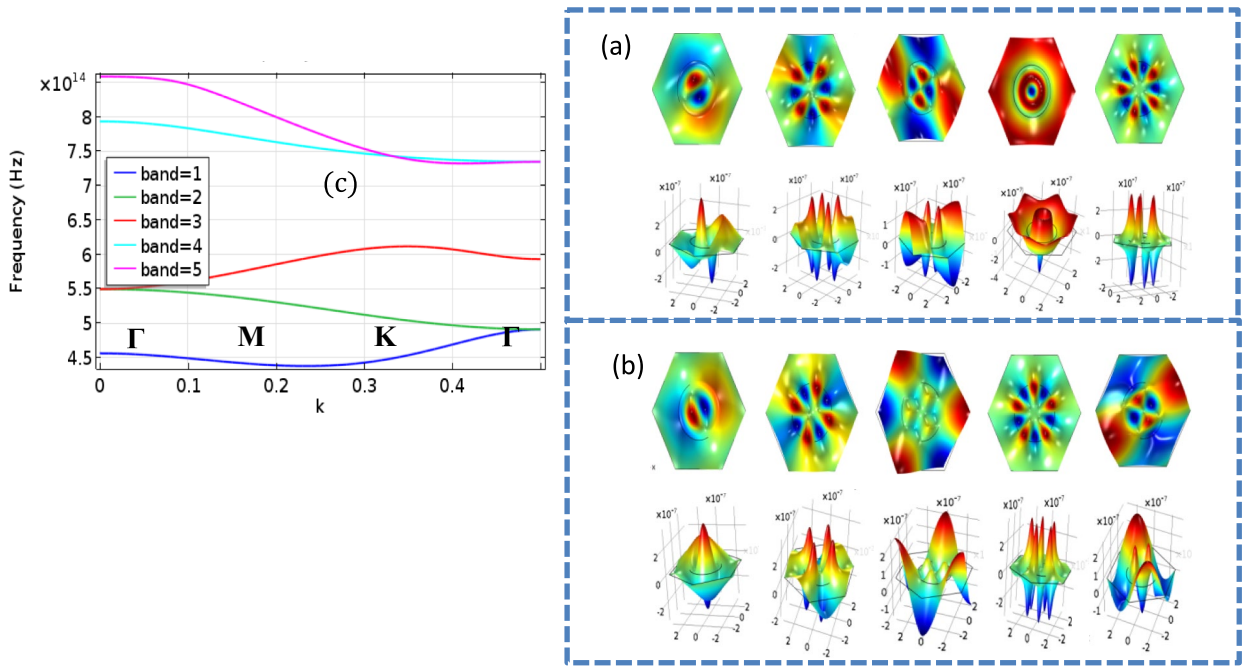

Fig. 4 Contour: Electric field norm (V/m) distribution for the first five eigenvalues of E_z modes in the unit cell of special symmetry points Γ, M, and K for the 1st BZ unit cell of hexagonal lattice (**a–b**), and in (**c**) the dispersion relation (**b** and diagram) of frequency as function the wavenumber k after swept from 0 to 0.5, show five photonic bands of unit cell in the hexagonal lattice, this structure shows one bandgap between the third and the four bands for TE- polarized wave can be clearly seen in the band diagram, although there is overlap in-band between the five and four bands. Shows there is no propagation of Bloch waves in this range of frequency that corresponds to the bandgap

will propagate in the waveguide with frequency inside the bandgap and confined to the linear defect area. This description happened when one row of rods is removed from the square lattice [1].

Simulation results and discussion

Point defect localized light in two square lattice photonic crystal

To begin, we are modelling a two-dimensional square photonic lattice with COMSOL software to remove a single rod from the band structure of a square lattice composed of dielectric rods gallium arsenide material (n = 3.48) is embedded in air (n = 1), with lattice constant a = 0.56 μm and rods radius r = 0.23a, as illustrated in Fig. 5a, which it represents the geometric design of the structure and hence the input and output characteristics of the light used during the square lattice crystal structure. While Fig. 5b, represents the type of mesh chosen in this design. The numerical result showed that the Surface: electric field norm (V/m) and Surface: the electric field, z- component (V/m) in (c and d) and the Surface and Contour height expression of them in (e and f) for the wavelength 1.55 μm of a point defect / resonant inside bandgap formed as result of the removing a single rod from the square lattice, which shows the field is trapped as a single localized mode state around the point defect inside the bandgap and the light cannot escape but bounce in the defect area. In (g and h) the electric field

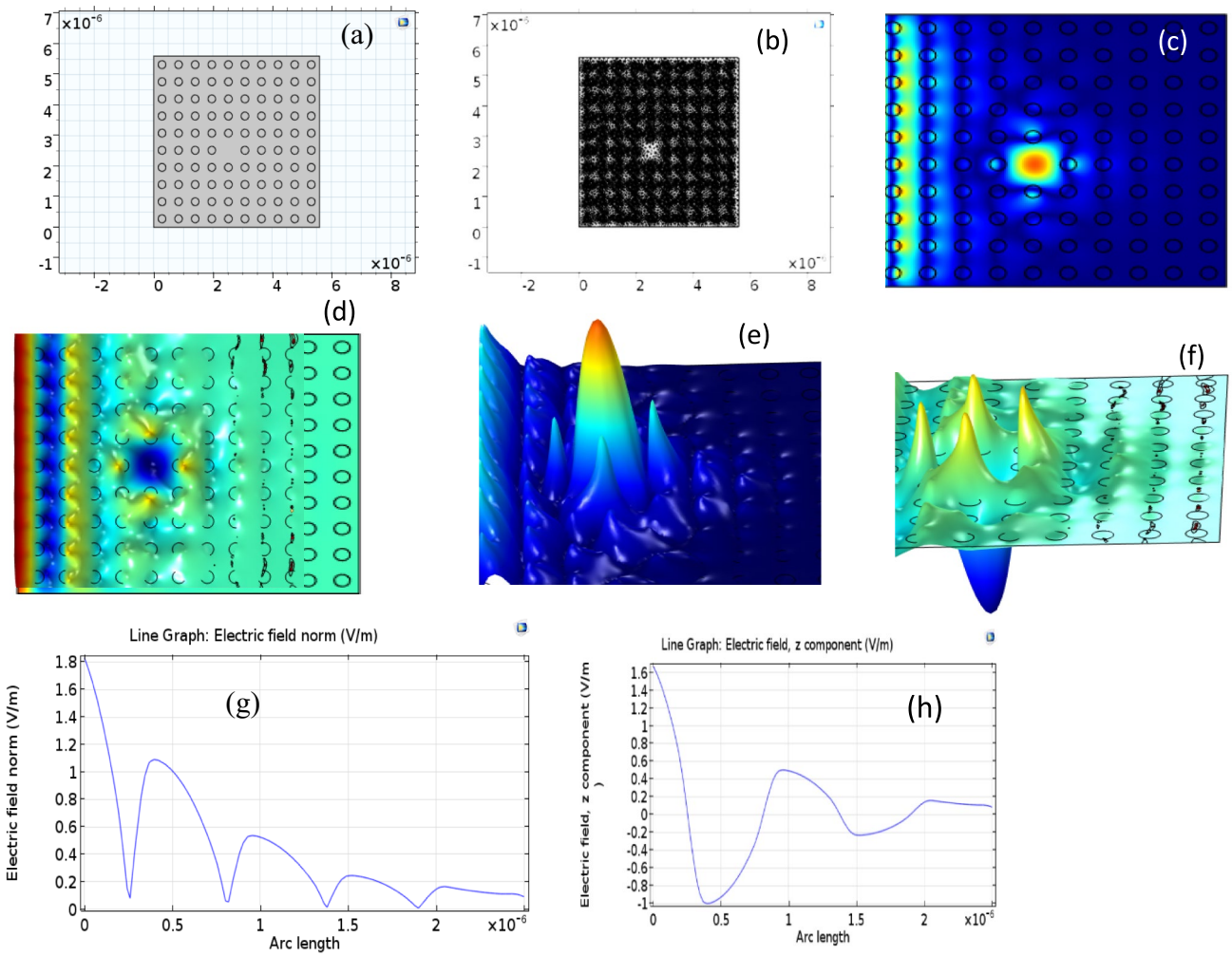

Fig. 5 The geometry of removing the single rod from the two-dimensional square lattice, lattice constant a = 0.56 μ*m* and the rods radius r = 0.23a in the air (**a**) Finite triangular element mesh (**b**) at the wavelength 1.55 μm. (**c**) The electric field norm (*E*) (**d**) the electric field (E_z) *z*-component (V/m) (**e** and **f**) Are the height expression of (E) and (Ez) which shows the localized mode about the defect in a square lattice; the field is trapped as a single localized mode state around the point defect inside the bandgap and it dissolves quickly as we move away from the defect site, this mode has a monopole state with single nodal plan formed defect and rotational symmetry with perfect crystal. In (**g** and **h**) the (E) and (E_z) in unit (V/m) as function to the Arc length

norm (V/m) and Electric field, z-component (V/m) as function to the Arc length, this defect in the cavity supports one mode consisting of frequency $\omega a/2\pi c = a/\lambda$ =0.361 for the wavelength 1.55 µm, we observe the fields bouncing back and forth through the defect, so light cannot escape and is trapped around the defect, the mode degrades dramatically in the photonic crystal. In fact, theoretical modeling using COMSOL software shows the results visually interesting and intuitive with respect to the resonant cavity, this design can be exploited and may be useful for light control applications within a narrow frequency band.

As well as show the field is concentered in the point cavity and rapidly decay as moving far from the defect site. Despite the creation of a defect within the lattice that breaks the crystal's translational symmetry. To enable the crystal to restore the same point symmetries, a variety of imperfections are still present. In our model we have proven this, we show after taking out a single rod from the photonic lattice, the rotational symmetry property is remained unchanged for the lattice, this means that we can stay rotate by 90° about the z-axis. Now, trying to model other simulations to predict other types of defects in square lattice photonic crystal by just adjusting the rod radii to r = 0.108a. By decreasing the rod radius, a wide fundamental gap between the first and second bands is obtained, see Fig. 6a, b. The numerical findings revealed a sharp peak centered at the resonant cavity and demonstrated that the localized mode is tightly confined to the defect by a broad bandgap between the first and second band as seen in Fig. 6c, d. Figure 6e, f shows the electric field norm (V/m) and the electric field (Ez) of z component (V/m) as function to the Arc length.

This mode monopole state formed defect (with a single nodal plane and high symmetry) is pushed up from the dielectric band. This finding is helpful because, in most cases, one can work as close to the maximum localized mode centered on the point defect as possible with a wide gap. For modeling the large rod radii, such as r = 0.34a, 0.44a and 0.55a as shown in Figs. 7, 8, and 9, Consequently, higher-order modes with a greater number of planes initially draw into the bandgap's gap, the different types of defect of higher-order modes depending on the amount of increase of rod radii, such as dipole, hexapole and high-order states of dipole are doubly degenerate, while other like quadruple and of high-order states of monopole is non-degenerate states [30]. The high-order modes appear in Figs. 7 and 8a and b when the rod radii are increased to r = 0.34 and 0.44, respectively. These dipole states are doubly degenerate and formed by a 90° rotation. On Fig. 9, when the rod radii are

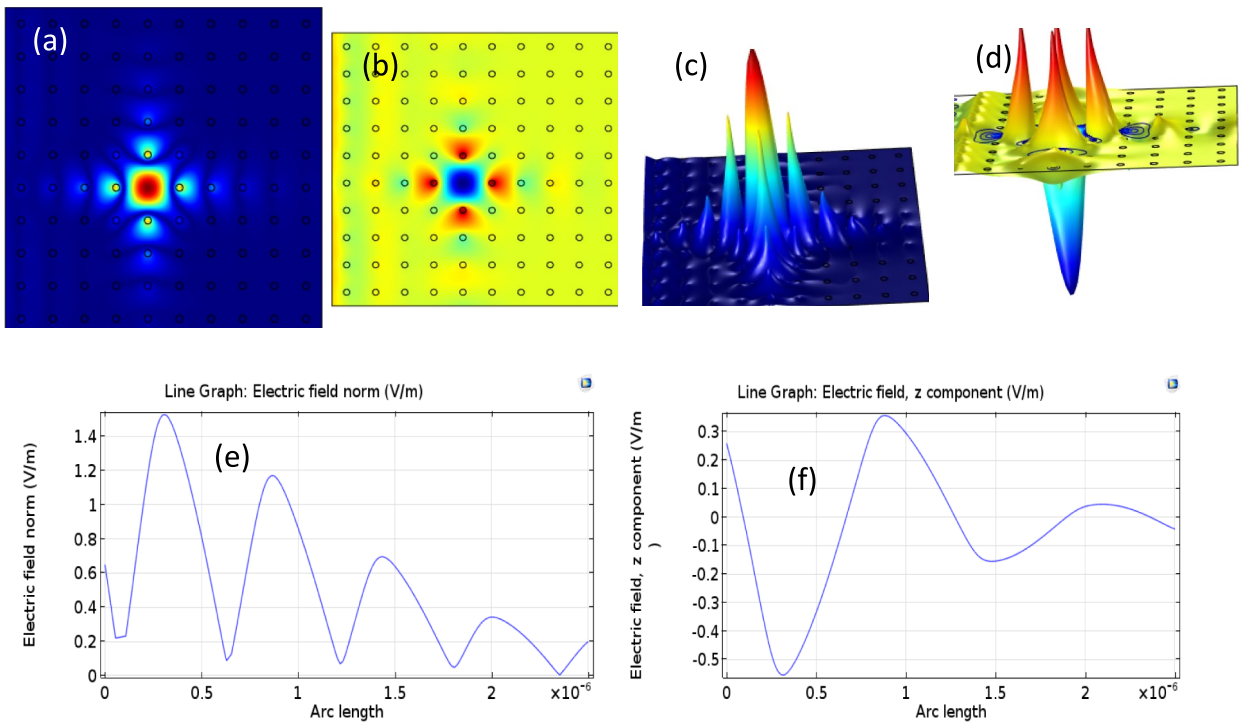

Fig. 6 Electric field norm (E) and the electric field (E_z) of z component (V/m) in (**a** and **b**), and the height expression of them in (**c** and **d**) of removing single rod from the two-dimensional square lattice with the lattice constant 0.56 µm and small rod radii r = 0.108a in air, show the localized mode are strongly confined about the defect by a wide bandgap, see also the sharp peak centered at the resonance cavity. This mode monopole state formed defect (with a single nodal plan and high symmetry) is pushed up from the dielectric band. In (**e** and **f**) the electric field norm (V/m) and the electric field (Ez) of z component (V/m) as function to the Arc length

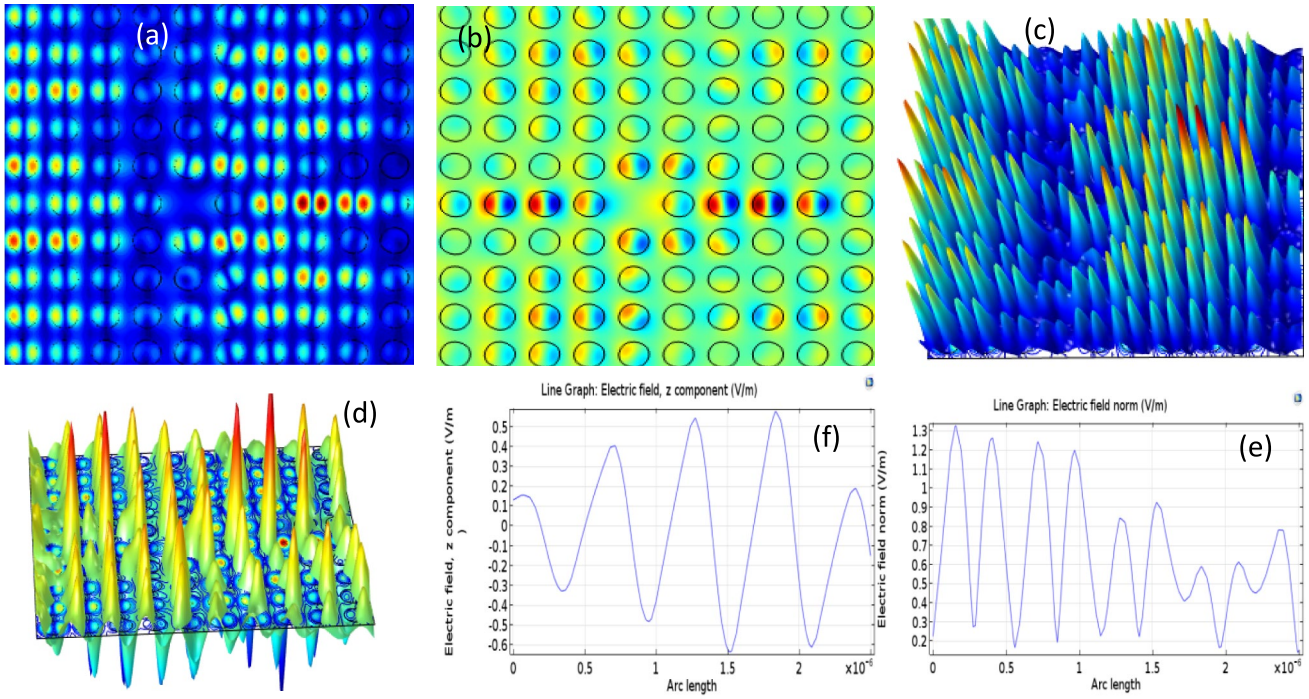

Fig. 7 Electric field norm (E) and the electric field z component (E_z) (V/m) in (**a** and **b**), and the height expression of them in (**c** and **d**) of removing single rod from the two-dimensional square lattice with the lattice constant a = 0.56 μm and large rod radii r = 0.34a in air, show the high-order appears as dipole state is doubly degenerate which formed by 90° rotation. In (**e** and **f**) the electric field norm (V/m) and the electric field (E_z) of z component (V/m) as function to the Arc length

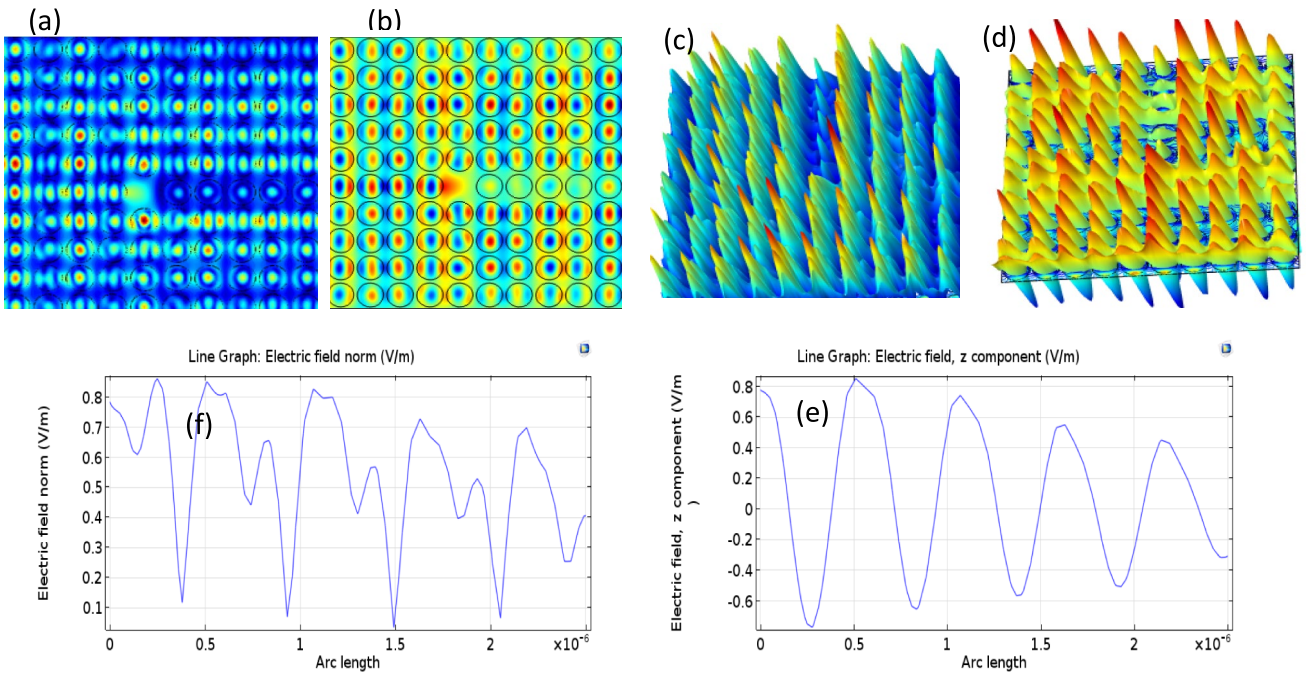

Fig. 8 Electric field norm (E) and the electric field z component (E_z) (V/m) in (**a** and **b**), and the height expression of them in (**c** and **d**) of removing single rod from the two-dimensional square lattice with the lattice constant a = 0.56 μm and large rod radii r = 0.44a in air, show the high-order appears as dipole state is doubly degenerate which formed by 90^0 rotation. (**e**, **f**) represent (E) and (E_z) respectively, as function to the Arc length

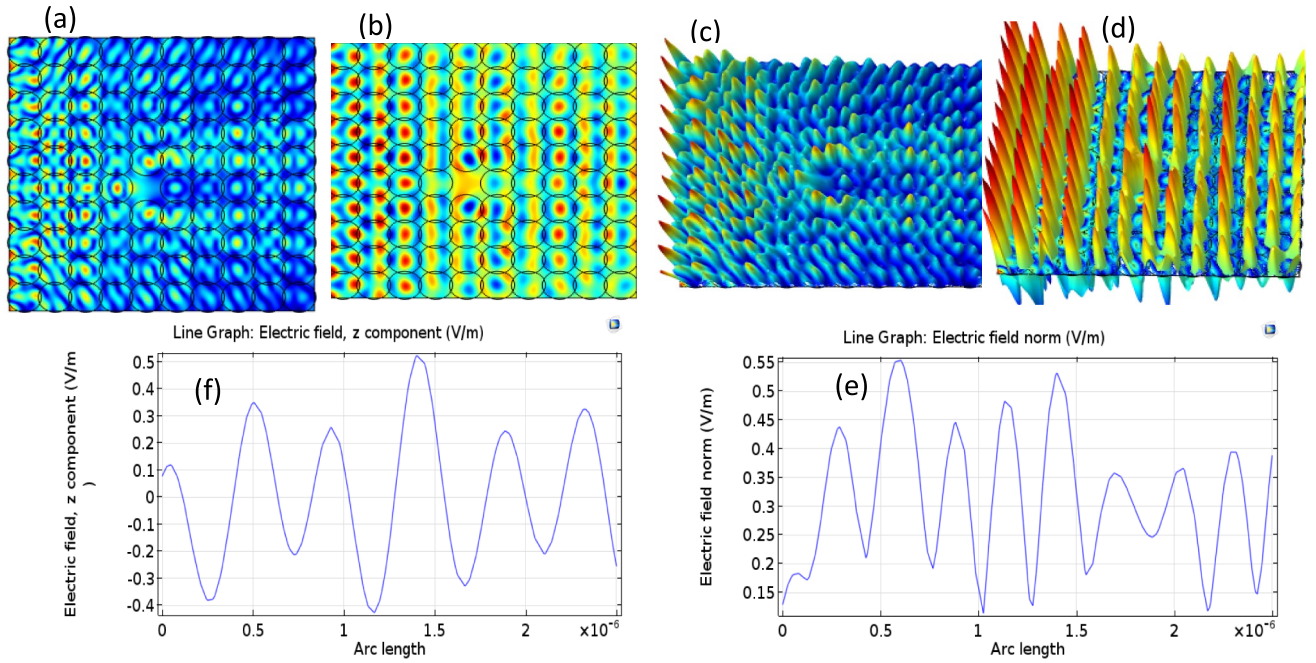

Fig. 9 Electric field norm (E) and the electric field z component (E_z) (V/m) in (**a** and **b**), and the height expression of them in (**c** and **d**) of removing single rod from the two-dimensional square lattice with the lattice constant a = 0.56 μm and large rod radii r = 0.55a in air, show appear two state the quadrupole states and the second- order monopole states with an extra node in the radial direction, these states are non-degenerate states. (**e**, **f**) represent (E) and (E_z) respectively, as function to the Arc length

increased to r = 0.55, two states appear, one of which is a quadrupole state and the other is a second-order monopole state with an additional node in the radial direction. These states are non-degenerate states.

Next, we are modeling a hexagonal lattice with the aid of COMSOL program, the same procedures we follow in the formation of point defects within the bandgap of the photonic crystal to create a single localized state within the bandgap. By removing a single rod from the 2D square lattice with a = 0.685 μm and small rod radius r = 0.2256a in air. Figure 10a represents the geometry of hexagonal lattice, Fig. 10b represent the finite element triangular mesh. Figure 10c, d represent the numerical result showed that the electric field norm (E) and (E_z) the electric field z-component of monopole state respectively, formed as result of the removing a single rod. Figure 10 (e, f) shows the field trapped as a single localized mode state around the point defect inside the bandgap and the light cannot escape but bounce in the defect area, the rotational symmetry property. Figure 10 (g, h) shows the electric field norm and the electric field z-component as function to the Arc length. The results show the monopole state formed as result the removing a single rod and this defect in the cavity supports one single mode consisting of frequency $\omega a/2\pi c = a/\lambda$ =0.4419 for the wavelength 1.55 μm. This result is helpful because, in most cases, a large gap can be used to get the maximum localized mode centered on the point defect.

Now, trying to simulate another photonic crystal with large rod radius to predict other types of defects, such as the higher-order modes. Increasing the number of planes initially pulls down into the gap within bandgap in hexagonal lattice photonic crystal by just adjusting the rod radii to r = 0.525a, 0.71a and 0.86a, as shown in Fig. 11. The numerical results showed different types of defects of higher-order modes. For rod radius of r = 0.525a formed the dipole states have doubly degenerate state. While increasing to r = 0.71a formed the second-order monopole states with the nodal plane in the radial direction are non-degenerate states, and the second–order dipole states are doubly degenerate with other states. By increasing to r = 0.86a formed a second-order monopole states, which are non-degenerate states with nodal plane in the radial direction. Dipole states have doubly degenerate with the other state, second–order dipole states are doubly degenerate with other states and the quadrupole states are non-degenerate states with nodal planes lying along the-x and-y axes and quadrupole-diagonal states are non-degenerate states with diagonal nodal planes.

We conclude from the creating of a point defect within both square and hexagonal lattice, that the electric field is well localized and trapped around the defect with high amplitude, and then we observe the decay of the field amplitude as we move away from the defect area. In both lattices, the mode defect appears to be monopole state with

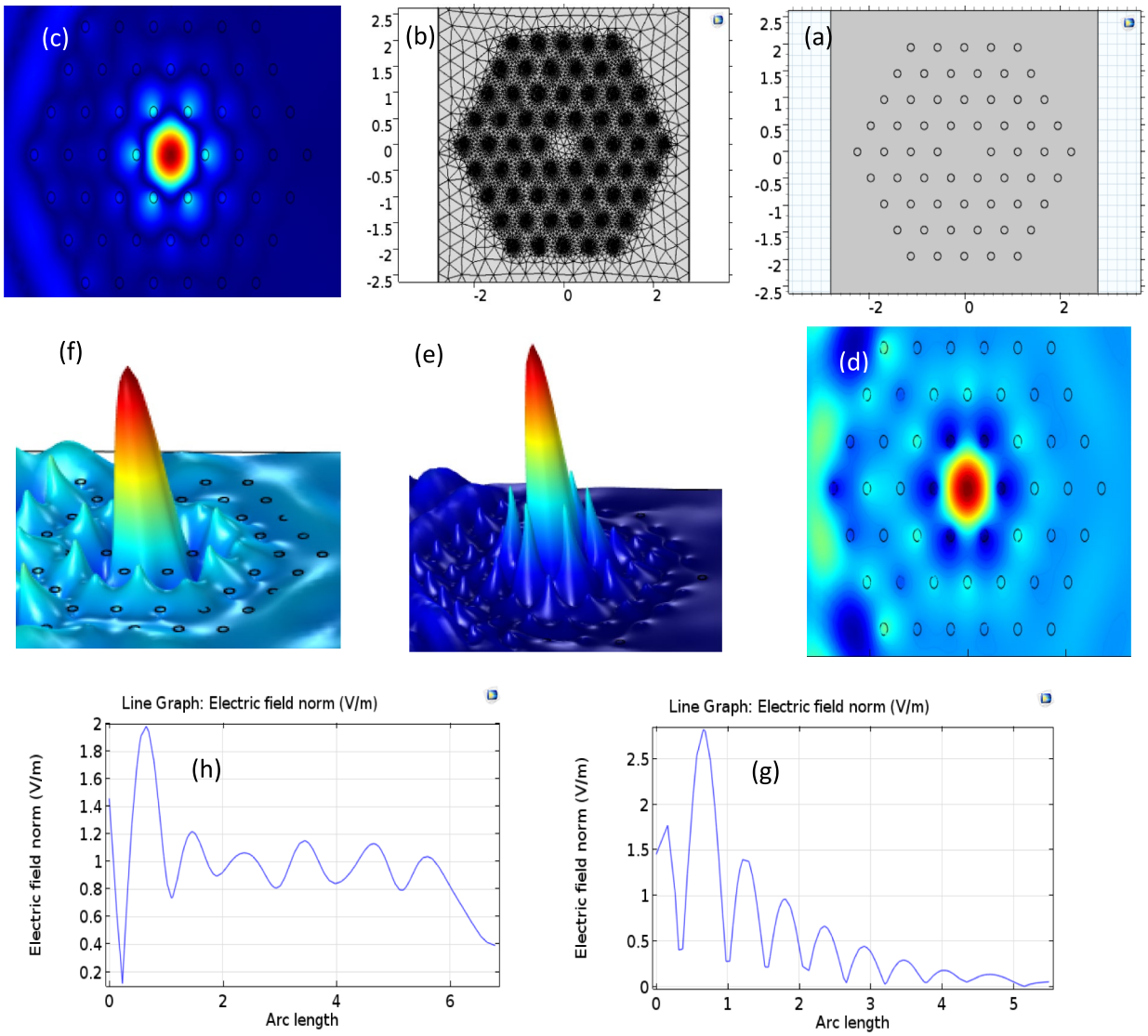

Fig. 10 (**a**) The geometry of removing the single rod from the 2D hexagonal lattice, with the a = 0.685 μ*m* and the rods with radius r = 0.2256a in the air (**b**) the finite triangular element mesh at the wavelength 1.55 μm. (**c** and **d**), the electric field norm (*E*) and the electric field (E_z) *z*-component respectively, (**e** and **f**) the height expression of both (*E*) and (E_z) respectively. The sharp peak centered at the resonance cavity. This mode monopole state formed defect (with a single nodal plane and high rotational symmetry) is pushed up from the dielectric band. (**g** and **h**) (*E*) and (E_z) respectively, as function to the Arc length

a single plane in the defect area and with rotational symmetry with a small rod radius [1]. In fact, we have been able to successfully design different types of localized states defects within the bandgap by increasing the rod radius, such as the dipole states, second-order monopole states, quadrupole states, and second-order dipole states, and determine the same important properties of photonic crystal, regardless of type of square or hexagonal lattice using COMSOL software. We additionally found that the modes appear to be the result of assembling localized states into a lattice.

Line defect localized light in two square and hexagonal lattice photonic crystals

Aiming to use COMSOL software simulation to model two-dimensional square and hexagonal photonic lattices in order to design the removal of a row of rods from the band structure of square and hexagonal lattices that are composed of dielectric rods of (n = 3.48) embedded in air (n = 1), with the lattice constants a = 0.68 μm and a = 0.542 μm and the rods with radius r = 0.2a and r = 0.256a respectively, as shows in Figs. 12 and 13a, b. Figures 12 and 13a show the geometric design for building

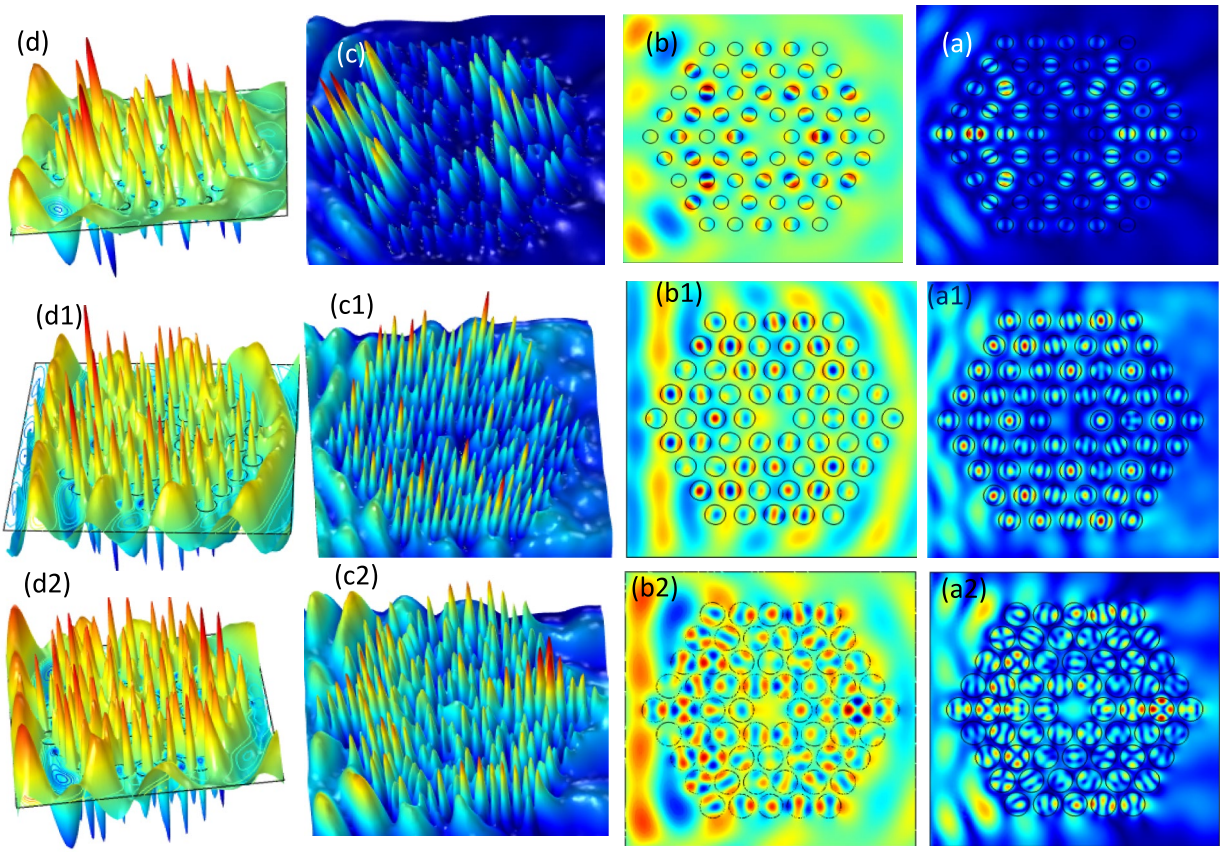

Fig. 11 (**a** and **b**) Electric field norm and the electric field $z-$ component respectively (**c** and **d**) the height expression of them in removing single rod from the 2D hexagonal lattice with a = 0.685 μ*m* and large rod radii r = 0.525a, r = 0.71a, r = 0.68a in air, (**c**, **d**) show the different localized states, such as dipole states are doubly degenerate with the other state when the radius increase to 0.525a. (a1, b1, c1 and d1) The second-order monopole states are non-degenerate states and the second order dipole states are doubly degenerate with other states for r = 0.71a. (a2,b2,c2 and d2) for r = 0.86a the different states, such as the second-order monopole states are non-degenerate states, dipole states have doubly degenerate with the other state, second– order dipole states are doubly degenerate with other states and the quadrupole states are non-degenerate states and quadrupole-diagonal states both are non-degenerate states with diagonal nodal planes

a linear defect inside the crystal with a square and hexagonal structure. While Figs. 12 and 13b shows choosing the appropriate mesh for engineering design. The numerical result showed that the (E) and (E_z) with linear defect is formed by removing row of rods to create a line defect to make a path to guide the light inside the band gape in one direction within the plane for which discrete guided translation symmetry as shown in Figs. 12 and 13c, d. Figures 12 and 13e, f shows the height expression of (E) and (E_z) for wavelengths 1.55 μm, in creating a line defect to make a path to guide the light inside the band gape in one direction. The results show in the figures a single guided mode inside the band gap by a single curved waveguide in a square and hexagonal photonic crystal composed of frequencies $\omega a/2\pi c = a/\lambda = 0.438$ and 0.349 for square and hexagonal lattices respectively. While the Figs. 12 and 13g and h, represent the electric field norm (V/m) and the electric field (E_z) of z component (V/m) as function to the Arc length.

Linear defect modeling demonstrates the photonic crystal ability to guide the light in one direction. By removing row of rods resulting in single-mode waveguide; it has the property of most single-mode being guided at a given frequency within the band structure. On the other hand, create a linear defect that produces a discrete guided band, the mode represented by that band is evanescent inside the photonic crystal and at the same time trapped inside the defect. In other words, outside of the bandgap, the modes are extended within the crystal, and inside the bandgap, the localized state of the defect area is introduced.

These features determine how the electric field is confined or steered within the photonic crystal for both point and line defects. The presence of flaws can cause the production of defect states, which can be seen in field plots as localized enhancements or changes in field distribution. The lattice configuration (square or triangular) affects the photonic band structure and, as a result, the field patterns surrounding the flaws.

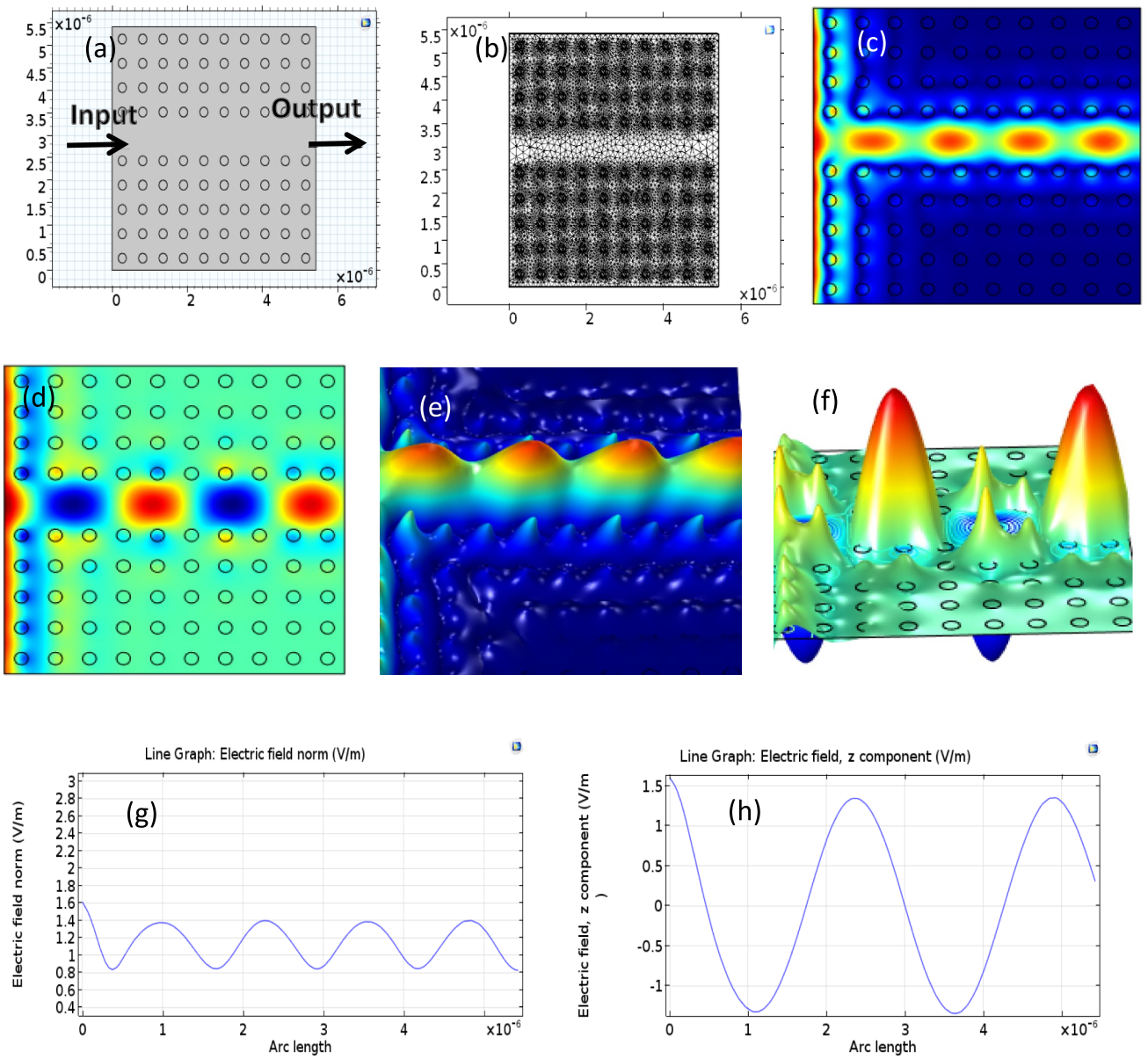

Fig. 12 The geometry of removing the row from the two-dimensional square lattice to carve a waveguide out of perfect photonic crystal, with the lattice constant 0.68 μm, and the rods radius r = 0.2a in the air for square lattice (**a**) and finite triangular element mesh (**b**) at the wavelength 1.55 μm. In (**c** and **d**), the electric field norm (E) and the electric field (E_z) of z-component (V/m) and the height expression of them in (**e** and **f**), carve a line defect to create a path to guide the light inside the band gape in one direction. In (**g** and **h**) the electric field norm (E) (V/m) and the electric field (E_z) of z component (V/m) as function to the Arc length

Conclusions

From the result, we were able to determine the main difference theoretically between the point defect and linear defect of both square and hexagonal photonic lattice. For the point defect, the mode is trapped wherever its frequency is within the band structure. As for the linear defect, the mode is localized to one direction propagation along with the defect, serving as a channel along where the light is propagated, rather than just a space that traps light. In addition, when creating a point defect inside the bandgap, the amplitude of the electric field is large and concentrated around the defect region and decays quickly as we move away from the site of the defect. While creating a line defect inside the bandgap, the amplitude of the electric field will continue to propagate in one direction to the end of the path of the line defect within the photonic crystal bandgap.

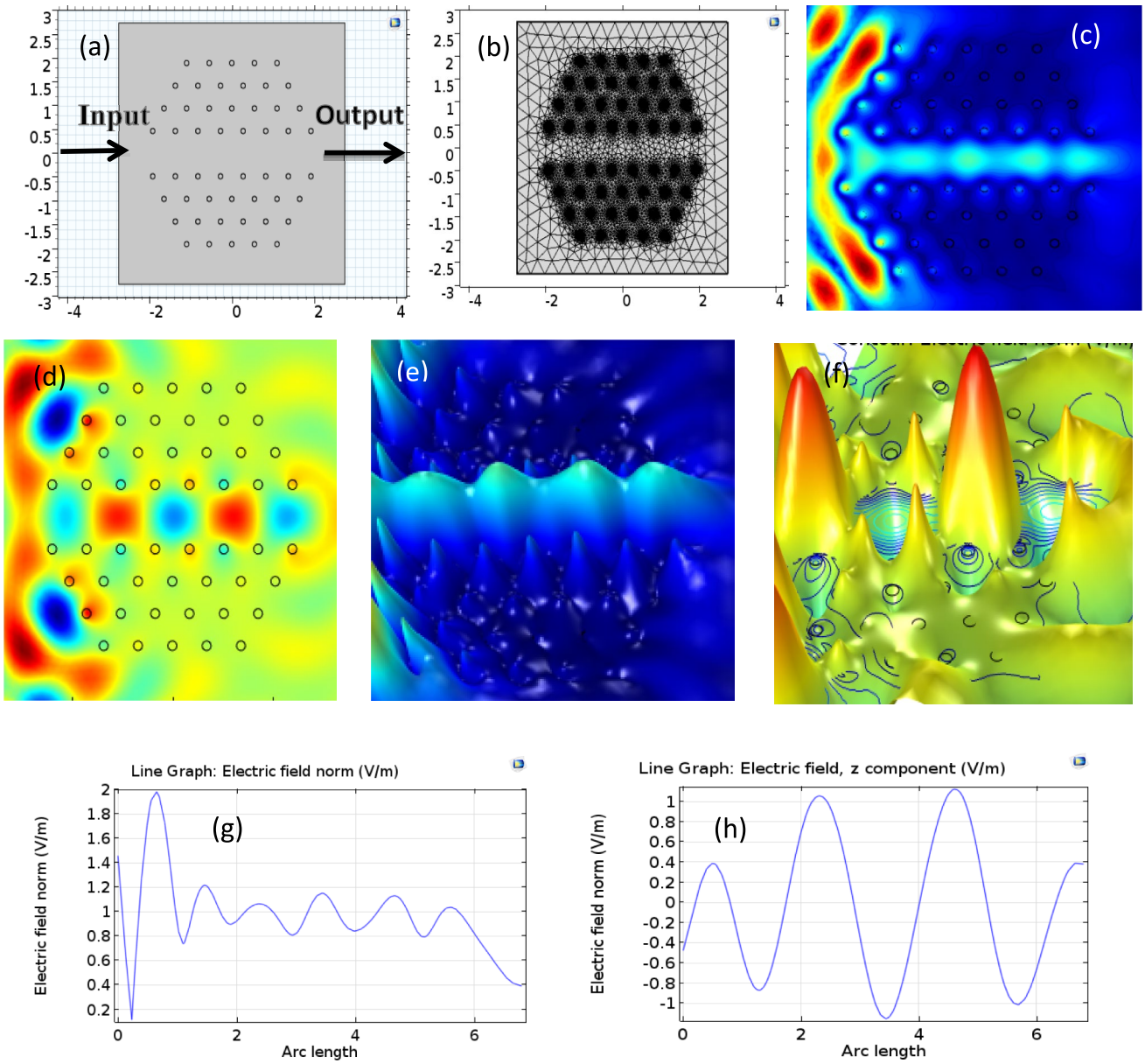

Fig. 13 The geometry of removing the row from the two-dimensional hexagonal lattice to carve a waveguide out of perfect photonic crystal, with the lattice constant 0.542 μ*m*, and the rods radius r = 0.256a in the air for hexagonal lattice (**a**) and finite triangular element mesh (**b**) at the wavelength 1.55 μm. In (**c** and **d**), the electric field norm (E) and the electric field (E_z) of z-component (V/m) and the height expression of them in (**e** and **f**), carve a line defect to create a path to guide the light inside the band gape in one direction. In (**g** and **h**) the electric field norm (E) (V/m) and the electric field (E_z) of z component (V/m) as function to the Arc length

References

1. J.D. Joannopoulos, S.G. Johnson, R.D. Meade, J.N. Winn, *Photonic crystals: molding the flow of light*, 2nd edn. (Princeton University Press, New Jersey, 2008)
2. S. Shaari, A.J.M. Adnan Photonic crystal multiplexer/demultiplexer device for optical communication. Front. Guid. Wave. Opt. Optoelectron., (2010)
3. I. Andonegui, A.J. Garcia, The finite element method applied to the study of two-dimensional photonic crystals and resonant cavities. J. Opt. express. **21**, 4072–4092 (2013)
4. Y. Zhe, C. Kan, W. Chen-ge, S. Xuan, L. Nan, S. Xiao-wu, A photonic crystal beam splitter used for light path multiplexing: synergy of TIR and PBG light guiding. J. Opt. Quantum. Electron. **52**, 2 (2020)

5. S.L. McCall, P.M. Platzman, R. Dalichaouch, D. Smith, S. Schultz, Microwave propagation in two-dimensional dielectric lattices. J. Phys. Rev. Lett. **67**(15), 2017–2020 (1991)
6. M. Mohammed, A.K. Ahmad, Numerical analysis of strongly coupled multicore photonic crystal fibres for multiplexer and de-multiplexer applications. J. Phys. Conf. Ser. **2322**, 012077 (2022)
7. M. Mohammed, W. Cel, Photonic crystal analysis for multiplexer and de-multiplexer applications. J. Phys. Conf. Ser. **2322**, 012074 (2022)
8. B. Wang, M.A. Cappelli, A plasma photonic crystal bandgap device. Appl. Phys. Lett. **108**, 161101 (2016). https://doi.org/10.1063/1.4946805
9. M. Neisy, M. Soroosh, K. Ansari-Asl, All optical half adder based on photonic crystal resonant cavities. J. Photonic. Netw. Commu. **35**(2), 1–6 (2018). https://doi.org/10.1007/s11107-017-0736-6
10. O. Oltutul, S. Simsek, A.M. Mamedov, E. Ozbay, Phononic band gap and wave propagation on polyvinylidene fluoride-based acoustic metamaterials. J. Cogent. Phys. **3**(1), 1169570 (2016)
11. Waveguide bends in photonic crystals, http://ab-initio.mit.edu/photons/bends.html
12. Photonic crystal, https://www.comsol.com/model/photonic-crystal-14703
13. Maysenhölder W. Bloch waves in an infinite periodically perforated sheet, Proc. Int. Conf. on COMSOL in Munich, OCT. 12–14 (2016)
14. Tushar Biswas, Shyamal K. Bhadra, Electromagnetic wave guidance mechanisms in photonic crystal fibers, Proc. Int. Conf. on COMSOL in Pune, (2015)
15. N. Myoung, H.C. Park, A. Ramachandran, E. Lidorikis, R.J. Wan, Flat-band localization and self-collimation of light in photonic crystals. Sci. Rep. **9**, 2862 (2019)
16. B. Suthar, A. Bhargava, Structural effects on the photonic band structure of two dimensional photonic crystal. Int. J. Pure. Appl. Phys. **6**(1), 31–36 (2010)
17. W. Jin, Y.L. Xue, Optical fabrication of wavy lattices and photonic lattices with defects in photorefractive crystal by single step projection method. J. Superlattices. Microstruct. **82**, 136–142 (2015)
18. S. Naghizade, S.M. Sattari-Esfahlan, An optical five channel demultiplexer-based simple photonic crystal ring resonator for WDM applications. J. Opt. Commun. **41**, 37–43 (2020)
19. Asghar Askarian, Performance analysis of all optical 2×1 multiplexer in 2D photonic crystal Structure, J. Opt. Commun., https://www.degruyter.com/document/doi/https://doi.org/10.1515/joc-2021-0235/html
20. G.S.R. Dalai, S. Sandip, K. Santosh, Design of photonic crystal based compact all-optical 2×1 multiplexer for optical processing devices. J. Microelectron. **112**, 105046 (2021)
21. A. Asghar, Design and analysis of all optical half subtractor in 2D photonic crystal platform. Optik. **228**, 166126 (2021)
22 Massoudi Radhouene, M.K. MoniaNajjar, S Robinson Chhipa, B. Suthar, Design and analysis a thermo-optic switch based on photonic crystal ring resonator. Optik. **172**, 924–929 (2018). https://doi.org/10.1016/j.ijleo.2018.07.118
23. A. Asghar, A. Gholamreza, A novel proposal for all optical 2×4 decoder based on photonic crystal and threshold switching method. Opt. Quant. Electron. **54**, 1–15 (2022)
24. E. Veisi, M. Seifouri, S. Olyaee, A novel design of all-optical high speed and ultra-compact photonic crystal AND logic gate based on the Kerr effect. J. Appl. Phys. B. **127**, 70 (2021)
25. P. Sharan, T.A. Alrebdi, A. Alodhayb et al., Design of two-dimensional photonic crystal defect microcavity sensor for biosensing application. SILICON **15**, 5503–5511 (2023). https://doi.org/10.1007/s12633-023-02448-w
26 M.K. Chhipa, B.T.P. Madhav, B. Suthar et al., Ultra-compact with improved data rate optical encoder based on 2D linear photonic crystal ring resonator. Photon. Netw. Commun. **44**, 30–40 (2022). https://doi.org/10.1007/s11107-022-00975-x
27. M.K. Chhipa, B.T.P. Madhav, B. Suthar, Design and analysis of optical filter for optical communication networks using photonics technology. AIP. Conf. Proc. **2220**, 050020 (2020). https://doi.org/10.1063/5.0001249
28. M.K. Chhipa, B.T.P. Madhav, B. Suthar, An all-optical ultra-compact microring-resonator-based optical switch. J. Comput. Electron. **20**, 419–425 (2021). https://doi.org/10.1007/s10825-020-01628-w
29. M.K. Chhipa, B.T.P. Madhav, S. Robinson, V. Janyani, B. Suthar, Realization of all-optical logic gates using a single design of 2D photonic band gap structure by square ring resonator. Opt. Eng. **60**(7), 075104 (2021). https://doi.org/10.1117/1.OE.60.7.075104
30. J.I.N. Wei, J.U. Jian, H.O. Hoi Lut, H.O.O. Yeuk Lai, A. Zhang, Photonic crystal fibers, devices, and applications. J. Front. Optoelectron. **6**(1), 3–24 (2013)